Development 130, 1681-1690

doi:10.1242/dev.00367

DEVELOPMENT AND DISEASE

Defective somite patterning in mouse embryos with reduced levels of *Tbx6*

Phillip H. White, Deborah R. Farkas, Erin E. McFadden* and Deborah L. Chapman†

Department of Biological Sciences, University of Pittsburgh, Pittsburgh, PA 15260, USA
*Present address: UC Davis School of Veterinary Medicine, Davis, CA 95616, USA
†Author for correspondence (e-mail: dlc7@pitt.edu)

Accepted 20 December 2002

SUMMARY

During vertebrate embryogenesis, paraxial mesoderm gives rise to somites, which subsequently develop into the dermis, skeletal muscle, ribs and vertebrae of the adult. Mutations that disrupt the patterning of individual somites have dramatic effects on these tissues, including fusions of the ribs and vertebrae. The T-box transcription factor, Tbx6, is expressed in the paraxial mesoderm but is downregulated as somites develop. It is essential for the formation of posterior somites, which are replaced with ectopic neural tubes in *Tbx6*-null mutant embryos. We show that partial restoration of *Tbx6* expression in null mutants rescues somite development, but that rostrocaudal patterning within them is defective, ultimately resulting in rib and vertebral fusions, demonstrating that Tbx6 activity in the paraxial mesoderm is required not simply for somite specification but also for their normal patterning. Somite patterning is dependent upon Notch signaling and we show that *Tbx6* genetically interacts with the Notch ligand, delta-like 1 (*Dll1*). *Dll1* expression, which is absent in the *Tbx6*-null mutant, is restored at reduced levels in the partially rescued mutants, suggesting that *Dll1* is a target of Tbx6. We also identify the spontaneous mutation *rib-vertebrae* as a hypomorphic mutation in *Tbx6*. The similarity in the phenotypes we describe here and that of some human birth defects, such as spondylocostal dysostosis, raises the possibility that mutations in *Tbx6* or components of this pathway may be responsible for these defects.

Key words: Mouse, Somitogenesis, Segmentation, T-box, *Tbx6*, *Dll1*, *rib-vertebrae*

INTRODUCTION

One of the defining features of vertebrate embryology is the segmentation of paraxial mesoderm into somites, which lie on both sides of the neural tube. Subsequently, in response to signals from the surrounding tissues, the somites undergo regional differentiation to form the dermomyotome dorsally and the sclerotome ventrally. These will later differentiate to form the dermis, skeletal muscle of the back, body wall and limbs, and the vertebrae and ribs (reviewed by Christ et al., 2000). During their formation, each somite is also divided into rostral and caudal (R-C) halves, such that cells in the rostral half are different molecularly and physically from cells in the caudal half (reviewed by Pourquie and Kusumi, 2001; Saga and Takeda, 2001). These R-C differences are initially required for the establishment of somite boundaries and later for the process of resegmentation. During resegmentation, the sclerotome region of the somites is divided and reorganized such that the caudal region of one somite fuses with the rostral portion of the next more posterior somite to ultimately form the vertebrae and ribs of the adult organism. Resegmentation results in the connection of a skeletal muscle group (which is derived from a single somite) to two consecutive vertebrae, thereby allowing for vertebral movement (Huang et al., 1996).

Notch signaling is essential for establishing and maintaining somite boundaries by setting up differences between R-C halves of somites; this occurs within the anterior presomitic mesoderm (PSM), prior to somite formation. Mutations in various components of the Notch signaling pathway disrupt the process of somite segmentation and the latter process of resegmentation (reviewed by Pourquie and Kusumi, 2001). For example, mutations in the human *DLL3*, a Notch ligand, results in spondylocostal dysostosis, which is characterized by hemivertebrae, rib fusions and deletions that together lead to short stature in the affected individuals (Bulman et al., 2000). Improper subdivision of the somites into R-C halves results most noticeably in the formation of fused ribs and vertebrae. It may also result in defective patterning of other tissues, in particular the peripheral nervous system (PNS). The neural crest-derived spinal ganglia migrate through the rostral halves of the somites, thus giving the PNS a segmental arrangement, so that disruption of R-C somite patterning disrupts the segmental arrangement of the PNS (reviewed by Bronner-Fraser, 2000).

The mouse T-box transcription factor *Tbx6* is expressed in the primitive streak and PSM, and is downregulated as the paraxial mesoderm segments to form the somite (Chapman et al., 1996). Gene targeting studies in mice revealed that Tbx6 is necessary for the formation of paraxial mesoderm posterior to the forelimb bud, which is replaced by ectopic neural tubes

in the *Tbx6*-null mutant embryos (Chapman and Papaioannou, 1998). Primitive streak markers *T*, *Wnt3a* and *Fgf8* are all expressed in the *Tbx6*-null mutant, while PSM markers such as *Notch1* and paraxis are not, suggesting that differentiation of primitive streak into PSM is blocked (Chapman and Papaioannou, 1998) (D.L.C., unpublished).

The Notch ligand, delta-like 1 (*Dll1*) is expressed in the primitive streak and PSM, in a domain that overlaps with *Tbx6* (Bettenhausen et al., 1995; Chapman et al., 1996). Like other genes that are normally expressed in the PSM, *Dll1* is not expressed in the *Tbx6*-null mutant embryos (Chapman and Papaioannou, 1998), suggesting that it might be a target of Tbx6. Alternatively, its expression may be lost simply because the PSM is not present in the mutant. Herein, however, we present data that supports Tbx6 functioning through Dll1 in patterning the somites. First, we show that reduction of *Tbx6* expression in embryos below heterozygous levels leads to fusions of the ribs and vertebrae, a characteristic shared by Notch signaling mutants. We further show that these malformed vertebrae are due to improper patterning of the somites along their R-C axis. Second, we demonstrate, not only that *Tbx6* genetically interacts with the classic mouse mutant *rib-vertebrae* (*rv*), but also that *rv* is a hypomorphic mutation in *Tbx6*. Finally, we show that *Tbx6* genetically interacts with *Dll1*, and that this, together with the absence of *Dll1* expression in *Tbx6*-null mutant embryos, suggest that Tbx6 is upstream of *Dll1* in the pathway leading to somite formation and patterning.

MATERIALS AND METHODS

Transgenic mice

An 8.8 kb *Xba*I fragment from the *Tbx6* genomic locus was cloned upstream of the *lacZ* reporter gene, p1229. This fragment contains the entire coding region of the *Tbx6* gene, along with 2.3 kb upstream and 2 kb downstream sequences. The reporter plasmid, p1229 (gift of M. Maconochie), consists of the β-globin minimal promoter, the *lacZ* gene and the polyadenylation sequence from SV40. The insert was excised from the plasmid, purified and injected into FVB/N fertilized eggs according to standard techniques (Hogan et al., 1994). Eggs were then transferred to recipient females and were either dissected at embryonic day (E) 10.5 to E12.5 or allowed to go to term. Two permanent transgenic lines, *Tg*(*Tbx6*)*46Dlc and Tg*(*Tbx6*)*130Dlc* (hereafter referred to as *Tg46* and *Tg130*), were established with this transgene.

Mice

The *Tbx6*^{tm1Pa} mice have previously been described and are maintained on a mixed C57Bl6/J 129Sv/Ev genetic background (Chapman and Papaioannou, 1998). *Dll1*^{tm1Gos} and *rib-vertebrae* (*rv*) mutant mice were obtained from Jackson Laboratories and are maintained on a C57Bl6/J background (Beckers et al., 2000b; Hrabe de Angelis et al., 1997; Nacke et al., 2000). The two *Tbx6* transgenic lines (*Tg46* and *Tg130*) are maintained on both FVB/N and a mixed genetic background. Genotyping of the *Tbx6* and *Dll1* mutant mice was performed as previously described (Chapman and Papaioannou, 1998; Hrabe de Angelis et al., 1997). The *rv* allele was genotyped by Southern blot analysis using a *Tbx6*-specific genomic probe that detects a polymorphism between the *Tbx6* wild-type and *rv* mutant alleles. Similarly the *Tbx6* transgene was detected using a *Tbx6*-specific probe by Southern blot analysis.

PCR and cloning of *rv* lesion

Genomic DNA from *rv/rv* and wild-type C57Bl6/J mice was used for PCR using the following primers designed from sequences obtained at Ensembl Mouse Genome Server: (forward) 5′- CATTCCCAAAA-CCCCATTGC -3′, (reverse) 5′- TGCCCCTTCACTCTCTCCATC -3′; and (forward) 5′- GTGTAGTTGAAATGTTCTCGGCG -3′, (reverse) 5′- CACAGTTCCTGGTTCTCCAAGC -3′. The PCR products were cloned and sequenced as described above.

Whole-mount in situ hybridization

Whole-mount in situ hybridization was performed as previously described by Wilkinson (Wilkinson, 1992) using antisense riboprobes for *Tbx6*, *Tbx18*, *Dll1*, *Dll3*. *Mesp2*, *Uncx4.1*, *Cer1*, neurofilament L and myogenin. Hybridization and washes were performed at 63°C.

X-gal staining

Embryos were dissected at the indicated times and stained for β-galactosidase activity with X-gal as previously described (Ciruna et al., 1997).

Skeletal preparations

Skeletons from embryos dissected at E14.5 and E15.5 were stained with Alcian Blue (staining the cartilage) and Alizarin Red (staining the bone) as described by Hogan et al. (Hogan et al., 1994), except that staining was performed simultaneously at 37°C. After staining, embryos were cleared in 1% KOH and stored in 1% KOH:glycerol (90:10).

RESULTS

Tbx6 transgene drives reporter gene expression in a *Tbx6*-specific domain

To understand the genetic pathway that leads to PSM formation, we are using a transgenic approach to identify the *cis*-acting regulatory regions of *Tbx6* and thereby the gene(s) regulating *Tbx6* expression. During these studies, we identified a *Tbx6* genomic fragment capable of driving the expression of a minimal promoter-*lacZ* reporter gene in a *Tbx6*-specific manner (Fig. 1). This *Tbx6* transgene contains the entire coding region of *Tbx6*, as well as upstream and downstream flanking regions (Fig. 1A). Embryos carrying this transgene had *Tbx6*-specific β-galactosidase staining in the primitive streak and PSM (Fig. 1B-D) along with staining extending into the somites, where *Tbx6* transcripts are not normally detected (compare Fig. 1D with normal *Tbx6* expression in Fig. 1E). This somite staining was almost certainly due to the perdurance of the β-galactosidase, as whole-mount in situ hybridization showed that *lacZ* transcripts were downregulated in the first somite formed (Fig. 1F).

Partial transgene rescue of the *Tbx6* mutant phenotype

The *Tbx6* transgene described above contained the entire *Tbx6*-coding region along with sequences capable of driving reporter gene expression in a *Tbx6*-specific spatial and temporal pattern. Two transgenic lines, *Tg*(*Tbx6*)*46Dlc and Tg*(*Tbx6*)*130Dlc* (hereafter referred to as *Tg46* and *Tg130*), were established and used in attempts to rescue the *Tbx6* mutant phenotype (Fig. 2). *Tbx6*-null embryos (*Tbx6*^{tm1Pa}/*Tbx6*^{tm1Pa}) can be distinguished at E9.5 by the lack of somites posterior to the forelimb bud and a bulbous tailbud (Chapman and Papaioannou, 1998). Both transgenic lines drove reporter gene expression in *Tbx6*-null embryos – hence in the absence of endogenous Tbx6 (Fig. 2B,C and data not shown). A single copy of the *Tg46* transgene

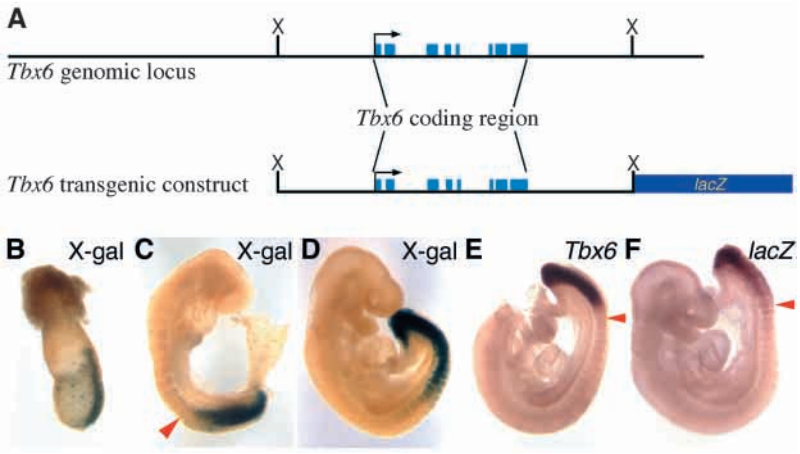

Fig. 1. *Tbx6* transgenic construct and expression pattern. (A) The *Tbx6* genomic locus (top) showing the positions of the exons (blue boxes), start of transcription (black arrow) and positions of the *Xba*I (X) sites used for cloning the *Tbx6* transgenic construct (bottom). The *Tbx6* transgenic construct consists of the entire coding region, upstream and downstream flanking regions and a *lacZ* reporter gene, which has a minimal promoter and a polyadenylation sequence. (B-D) Transgenic embryos, derived from the *Tg46* founder line, were dissected from E7.5-9.5 and stained for β-galactosidase activity. (B) Side view (posterior is towards the right) of an E7.5 mouse embryo showing X-gal staining predominantly within the primitive streak, but also widely scattered throughout the embryo. (C) By E8.5, staining is found within the primitive streak and PSM, with some stained cells found in the newly formed somites (red arrowhead). (D) Similarly, at E9.5, X-gal staining is seen in the primitive streak region and PSM, but also extending into the caudal-most somites. (E) Whole-mount in situ hybridization of endogenous *Tbx6* expression in an E9.5 wild-type embryo, showing the anterior limit of *Tbx6* transcripts in the PSM prior to somite segmentation (red arrowhead indicates the position of the newly formed somite). (F) Whole-mount in situ hybridization of *lacZ* expression in a *Tg46* transgenic embryo is largely limited to the primitive streak and PSM with transcripts downregulated in the newly formed somite (red arrowhead).

was able to rescue posterior somite formation in *Tbx6* mutant embryos. A noticeable feature of the $Tbx6^{tm1Pa}/Tbx6^{tm1Pa}$ *Tg46/+* mutants was an enlarged tailbud (albeit smaller than the tailbud of a *Tbx6* null mutant), which tended to branch at later times in development (Fig. 2B-D). Interestingly, β-galactosidase staining accumulated in the dorsal region of the enlarged tailbud (Fig. 2B,C). Incomplete rescue of the *Tbx6* mutant phenotype suggested that the levels of *Tbx6* expressed from the transgene might be reduced compared with normal embryos. Examination of *Tbx6* expression in the $Tbx6^{tm1Pa}/Tbx6^{tm1Pa}$ *Tg46/+* embryos revealed that although transcripts were present in both the primitive streak and PSM, they were found at lower than heterozygous levels (Fig. 2E), which could account for the incomplete rescue observed for this transgene. To examine the fate of somites formed in *Tg46* rescued embryos, litters were dissected from $Tbx6^{tm1Pa}/+$ *Tg46/+* × $Tbx6^{tm1Pa}/+$ matings at E15.5. At the level of gross morphology, *Tg46* rescued embryos can be distinguished by their short stature and short tails compared with control embryos (Fig. 2F,G). Skeletal preparations revealed severe fusions of the ribs and vertebrae along the axis, which may account for the short stature of the embryos (Fig. 2I). These embryos were still alive at E15.5, indicating that the transgene rescues the early embryonic lethality observed in the $Tbx6^{tm1Pa}/Tbx6^{tm1Pa}$ embryos, which are normally dead by E12.5. The *Tg46* rescued mutants, however, are dead at birth, perhaps due to the failure of the malformed ribs to protect internal organs during birth.

The second transgenic line, *Tg130*, was much less efficient at restoring somite formation in the *Tbx6* null. Approximately half of the $Tbx6^{tm1Pa}/Tbx6^{tm1Pa}$ *Tg130/+* embryos were similar in phenotype to the $Tbx6^{tm1Pa}/Tbx6^{tm1Pa}$ embryos and were resorbed by E15.5, while the remainder formed only a few fused ribs and vertebrae and died later in utero as they were never born (Fig. 2K). *Tbx6* is expressed at very low levels, if at all, in the $Tbx6^{tm1Pa}/Tbx6^{tm1Pa}$ *Tg130/+* embryos (data not shown). In attempts to increase the level of *Tbx6* expression, we also generated $Tbx6^{tm1Pa}/Tbx6^{tm1Pa}$ that were homozygous for the *Tg130* transgene. The $Tbx6^{tm1Pa}/Tbx6^{tm1Pa}$ *Tg130/Tg130* embryos displayed a range of phenotypes, some similar in phenotype to the $Tbx6^{tm1Pa}/Tbx6^{tm1Pa}$ *Tg130/+* embryos, forming only a few ribs and vertebrae, while others resembled the *Tg46* rescued *Tbx6* mutants, forming fused vertebrae and ribs and found still born (data not shown). Because the *Tg46* transgene is lethal when homozygous, we were unable to determine the effect of increasing *Tbx6* expression by generating $Tbx6^{tm1Pa}/Tbx6^{tm1Pa}$ *Tg46/Tg46* embryos. Instead, we increased *Tbx6* expression levels by combining both the *Tg130* and *Tg46* transgenes hemizygously in the *Tbx6* null. Although the $Tbx6^{tm1Pa}/Tbx6^{tm1Pa}$ *Tg46/+ Tg130/+* embryos still showed signs of rib fusions (Fig. 2L,M) they were much less severe than in embryos with only one copy of either transgene (compare Fig. 2L,M with 2I,K).

Rostrocaudal patterning of the somites is disrupted in *Tbx6* transgenic embryos

Through our attempts to rescue the *Tbx6* mutant using a transgene that expresses *Tbx6* at low levels, we have established a series of *Tbx6* phenotypes characterized by rib and vertebral fusions, which suggests improper patterning of the somites. To explore this possibility more carefully, we performed whole-mount in situ hybridization using markers of somite R-C patterning on *Tg46* rescued embryos and their littermates derived from crosses of $Tbx6^{tm1Pa}/+$ *Tg46/+* × $Tbx6^{tm1Pa}/+$ mice.

The paired homeobox gene *Uncx4.1* is normally expressed in the caudal halves of somites (Mansouri et al., 1997; Neidhardt et al., 1997) (Fig. 3A). In the $Tbx6^{tm1Pa}/Tbx6^{tm1Pa}$ *Tg46/+* embryo, *Uncx4.1* transcripts are detected throughout the somitic region with no apparent stripes (Fig. 3B,C). In some of these embryos, *Uncx4.1* appears as darker stripes in the most recently formed somites; however, these stripes are found amidst uniform, low-level *Uncx4.1* expression (Fig. 3D). Thus, somites in these partially rescued *Tbx6* mutants appear to be caudalized.

To explore further whether rostral somite compartments form in the *Tg46* rescued embryos, we examined the expression of several markers of rostral somite compartment

identity. The bHLH transcription factor, *Mesp2*, is normally expressed in the anterior PSM, initially in a domain that spans the width of a somite, but rapidly becoming localized to the rostral half of the forming somite (Saga et al., 1997). *Mesp2*-null embryos lose rostral somite compartment identity and the caudalized paraxial mesoderm fails to segment. Although *Mesp2* was not expressed in the *Tbx6*-null mutant, transcripts were present in the anterior PSM of both control and *Tg46* rescued embryos (Fig. 3E; data not shown), suggesting that rostral identity is not completely lost in these embryos. In some of the *Tg46* rescued embryos, a low level of *Mesp2* transcripts was detected in the most recently formed somite, in addition to expression in the anterior PSM. As Mesp2 is required to repress its own expression (Takahashi et al., 2000), this ectopic expression suggests that in at least some of these *Tg46* rescued embryos, Mesp2 fails to downregulate its own expression.

Mouse cerberus-related gene 1, *Cer1*, is expressed as two stripes in the anterior PSM and in the rostral region of the most recently formed somite (Biben et al., 1998; Shawlot et al., 2000) (Fig. 3F). As expected, *Cer1* is not expressed in the *Tbx6*-null mutant (data not shown). *Cer1* is expressed in the PSM of *Tg46* rescued embryos, but levels are reduced compared with control embryos, and no expression is detected in the newly formed somite (Fig. 3F). This result also suggests that rostral somite compartment identity of the PSM is initially observed; however, it is not maintained in these embryos.

Neural crest-derived spinal ganglia migrate through the rostral half of the sclerotome, therefore loss or improper

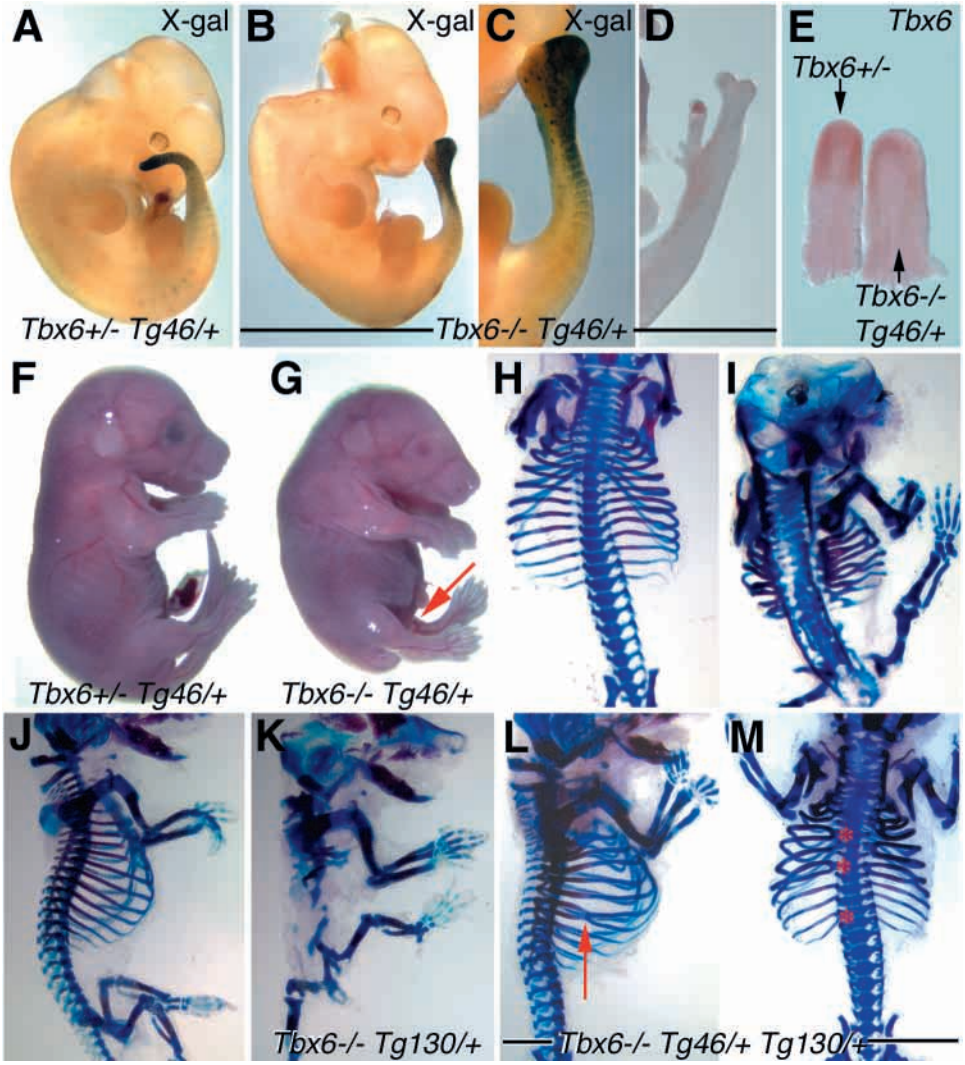

Fig. 2. Partial rescue of the *Tbx6* mutant phenotype with *Tbx6* transgenes. Embryos were dissected at E10.5 (A-C,E), E13.5 embryos (D), and E15.5 (F-M). Embryos were derived from the following crosses: *Tbx6*^{tm1Pa}/+ *Tg46*/+ × *Tbx6*^{tm1Pa}/+ (A-I), *Tbx6*^{tm1Pa}/+ *Tg130*/+ × *Tbx6*^{tm1Pa}/+ (J,K), and *Tbx6*^{tm1Pa}/+ *Tg46*/+ × *Tbx6*^{tm1Pa}/+ *Tg130*/+ (L,M). Genotypes are indicated in the panels with *Tbx6*$^{+/-}$ or *Tbx6*$^{-/-}$ denoting hetero- or homozygosity for the *Tbx6*^{tm1Pa} allele, respectively and *Tg46*/+ or *Tg130*/+ denoting hemizygosity for the *Tg46* or *Tg130* transgene, respectively. (A-C) X-Gal staining reveals predominant expression of the *Tg46* transgene in the tailbud, with perdurance of β-galactosidase in the formed somites of both control and *Tg46* rescued embryos. (B,C) A *Tg46* partially rescued *Tbx6* mutant, in which posterior somites are clearly seen in the high magnification of the tail region (C). X-gal staining is present in the caudal-most somites and predominantly in the dorsal region of the expanded tailbud. (D) Branching morphology of an E13.5 tail from a *Tg46* rescued embryo. (E) Whole-mount in situ hybridization of *Tbx6* expression in the tails of *Tbx6*^{tm1Pa}/+ and *Tbx6*^{tm1Pa}/*Tbx6*^{tm1Pa} *Tg46*/+ embryos, showing that although *Tbx6* is expressed in both the primitive streak and the PSM, transcripts are downregulated in the *Tg46* rescued embryos compared with the heterozygotes. (F,G) Gross morphological analysis reveals the short stature and short tail (red arrow indicates the tip of the tail in G) of the *Tbx6*^{tm1Pa}/*Tbx6*^{tm1Pa} *Tg46*/+ compared with the *Tbx6*^{tm1Pa}/+ *Tg46*/+ embryo. (H,I) Alcian Blue and Alizarin Red stained skeletons of the embryos pictured in F,G reveal fused vertebrae and fused ribs along the entire AP axis of the *Tbx6*^{tm1Pa}/*Tbx6*^{tm1Pa} *Tg46*/+ (I). Fusions of the ribs are detected in both proximal and more distal regions of the ribs. (J,K) Alcian Blue and Alizarin Red skeletal staining of embryos derived from a *Tbx6*^{tm1Pa}/+ *Tg130*/+ × *Tbx6*^{tm1Pa}/+ cross. *Tbx6*+/+ *or Tbx6*^{tm1Pa}/+ embryos with or without the *Tg130* transgene were indistinguishable (J), while *Tbx6*^{tm1Pa}/*Tbx6*^{tm1Pa} *Tg130*/+ embryos showed almost complete absence of vertebrae and ribs (K). (L,M) Side (L) and dorsal (M) views of a *Tbx6*^{tmPa1}/*Tbx6*^{tmPa1} *Tg46*/+ *Tg130*/+ embryonic skeleton showing more complete rescue of the mutant phenotype than with either transgene alone (compare L,M with I,K). Fusions were predominantly found in the cervical (not visible in these panels) and thoracic regions (red arrow in L and red asterisks in M), while the lumbar or sacral regions appeared normal.

formation of this somite compartment will lead to alterations in the appearance of the spinal ganglia. To investigate this, we examined the expression of neurofilament L, which is segmentally expressed in the spinal ganglia along the anteroposterior (AP) axis of normal embryos (Lewis and Cowan, 1985) (Fig. 3G). The rostral compartment of the somites is clearly disrupted in the *Tg46* rescued embryos as shown by the expression pattern of neurofilament L. In contrast

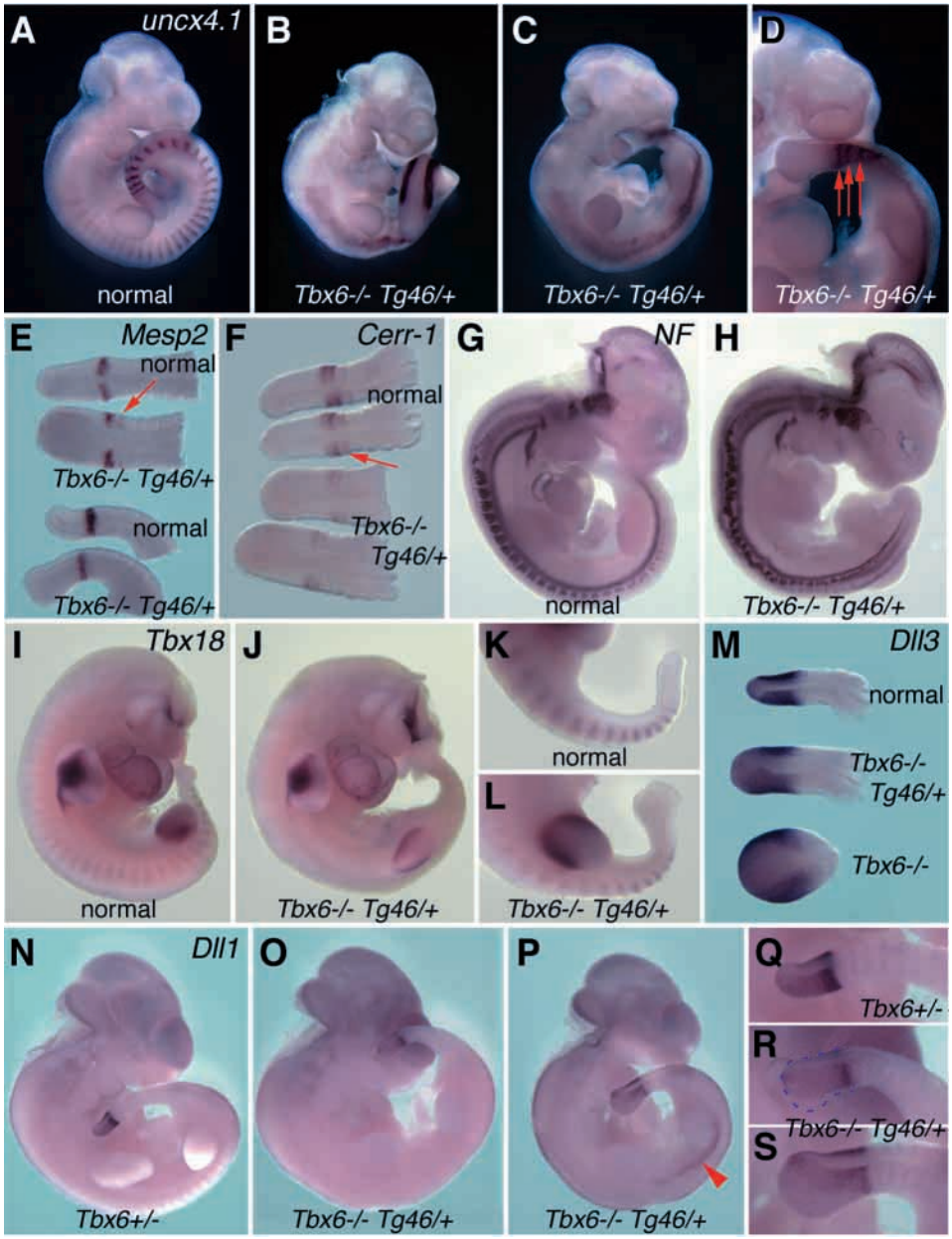

Fig. 3. Whole-mount in situ hybridization of *Tg46* rescued mutant embryos reveals abnormalities in R-C somite patterning. Embryos, derived from *Tbx6*^{tm1Pa}/+ *Tg46*/+ × *Tbx6*^{tm1Pa}/+ crosses, were dissected at E10.5 and hybridized with *Uncx4.1* (A-D), *Mesp2* (E), *Cer1* (*Cerr-1* in figure; F), neurofilament l (G-H), *Tbx18* (I-L), *Dll3* (M) and *Dll1* (H-M) antisense riboprobes. The genotypes of the embryos are as indicated. The designation of 'normal' is given to embryos that are wild type or *Tbx6*^{tm1Pa}/+ with or without the transgene, as no differences were observed between these genotypes when hybridized with the specified probes. (A) *Uncx4.1* is normally expressed in the caudal region of each somite along the AP axis. (B-D) By comparison, *Uncx4.1* transcripts are found throughout the somites of the *Tbx6*^{tm1Pa}/*Tbx6*^{tm1Pa} *Tg46*/+ embryos. (C,D) In some cases, the posterior-most somites express stripes of *Uncx4.1* transcripts; however, these stripes (red arrows in D) are found on a background of low uniform levels of *Uncx4.1* expression. (E) *Mesp2* is expressed in the rostral region of the forming somite in both normal and *Tbx6*^{tm1Pa}/*Tbx6*^{tm1Pa} *Tg46*/+ embryonic tails (dorsal view) at comparable levels. In the tail of the top *Tbx6*^{tm1Pa}/*Tbx6*^{tm1Pa} *Tg46*/+ embryo, very low levels of *Mesp2* transcripts are also detected in the last somite to form (red arrow). (F) *Cer1* is expressed as two stripes in the anterior PSM and in the rostral region of the newly formed somite (red arrow) in normal embryos. *Cer1* transcripts are downregulated in the anterior PSM and absent in the newly formed somite of *Tbx6*^{tm1Pa}/*Tbx6*^{tm1Pa} *Tg46*/+ embryos. (G) Neurofilament L (*NF* in figure) is expressed in the spinal ganglia and neural tube of normal embryos. Expression in the spinal ganglia appears as evenly distributed blocks along the axis, reflecting their migration route through the rostral halves of the somites. (H) By contrast, Neurofilament L expression in the spinal ganglia of the *Tbx6*^{tm1Pa}/*Tbx6*^{tm1Pa} *Tg46*/+ embryo is irregularly distributed along the axis, often appearing as fused blocks. (I-L) Lateral views of normal and *Tbx6*^{tm1Pa}/*Tbx6*^{tm1Pa} *Tg46*/+ embryos showing *Tbx18* expression. The heads of the embryos in have been removed for genotyping. *Tbx18* is normally expressed in the rostral halves of somites along the AP axis, as well as in the heart and limb buds (I,K). In the *Tbx6*^{tm1Pa}/*Tbx6*^{tm1Pa} *Tg46*/+ embryos, *Tbx18* is either not expressed in the paraxial mesoderm (J) or is expressed in the newly formed somites, eventually being lost in more anterior regions of the embryo (L). (M) Dorsal view of *Dll3* expression in the tailbuds of normal, *Tbx6*^{tm1Pa}/*Tbx6*^{tm1Pa} and *Tbx6*^{tm1Pa}/*Tbx6*^{tm1Pa} *Tg46*/+ embryos. (N,Q) In normal embryos *Dll1* is expressed in the tailbud and PSM, and is upregulated in the next-to-form somite. Low levels of *Dll1* are later detected in the caudal compartment of the formed somites (Q). (O,P,R,S) The level of *Dll1* transcripts in the tails of *Tbx6*^{tm1Pa}/*Tbx6*^{tm1Pa} *Tg46*/+ embryos is reduced compared with *Tbx6*^{tm1Pa}/+ embryos. Weak upregulation of *Dll1* expression can be seen in the anterior region of the PSM prior to somite segmentation. The expanded tail region of the *Tbx6*^{tm1Pa}/*Tbx6*^{tm1Pa} *Tg46*/+ embryos can be seen in R and S (broken blue outline in R), where *Dll1* transcripts appear dorsally localized. Low levels of *Dll1* transcripts are later localized to the caudal compartment of the formed somites similar to the *Tbx6*^{tm1Pa}/+ embryos. (P) *Dll1* expression in the flank of the *Tg46* rescued embryo marks ectopic neural tissue (red arrowhead).

to the segmented appearance of the neurofilament L-expressing spinal ganglia in the normal embryo, the segments are disorganized and often joined in rescued embryos (Fig. 3H).

The T-box gene *Tbx18* is expressed in the rostral region of somites along the AP axis of the embryo, in addition to the heart and limb buds (Kraus et al., 2001) (Fig. 3I,K). A range of expression patterns was observed for this gene in the *Tg46* rescued embryos. Some rescued embryos failed to express *Tbx18* in the somites (Fig. 3J), while other embryos expressed reduced levels of *Tbx18* transcripts in the rostral region of the newly formed somites, but this expression was not maintained in more anterior somites (Fig. 3L). In between these two extremes were embryos that expressed *Tbx18* at reduced levels and in smaller domains in the most newly formed somites. However, it was no longer expressed in more anterior regions of the embryo (data not shown). Altogether these marker gene studies show that R-C somite patterning is clearly disrupted in the *Tg46* rescued mutant embryos, with somites losing their rostral compartment identity.

Expression of *Dll1*, but not *Dll3*, is reduced in *Tbx6* transgenic embryos

The defect in R-C somite patterning in the $Tbx6^{tm1Pa}/Tbx6^{tm1Pa}$ *Tg46/+* embryos suggests that expression of one or more components of the Notch signaling pathway is disrupted in these embryos. Two Notch ligands, Dll1 and Dll3, are known to be involved in R-C somite patterning (Barrantes et al., 1999; Dunwoodie et al., 2002). *Dll3* is normally expressed in the primitive streak, PSM and later in the rostral somite compartment of the two most recently formed somites (Dunwoodie et al., 1997). In contrast to most PSM expressed genes, including *Dll1*, *Dll3* is expressed in the *Tbx6*-null mutant and its expression in the tailbud of the *Tg46* rescued embryos is comparable with controls (Fig. 3M). *Dll3* expression in the rostral regions of the newly formed somites of the *Tg46* rescued embryos is not apparent; however, expression in this domain was not seen in control embryos either (Fig. 3M).

Dll1 is normally expressed in the primitive streak and PSM, then localizing to the caudal halves of somites (Bettenhausen et al., 1995) (Fig. 3N,Q). Although *Dll1* is not expressed in the tail mesoderm of the *Tbx6*-null embryo (Chapman and Papaioannou, 1998), *Dll1* expression is restored in the $Tbx6^{tm1Pa}/Tbx6^{tm1Pa}$ *Tg46/+* embryos, with transcripts present in the PSM with a slight upregulation in the somite that is next to form (Fig. 3O,P). *Dll1* expression levels, however, were reduced in the *Tg46* rescued embryos compared with *Tbx6* heterozygotes (compare Fig. 3N,Q with 3O,P,R,S). Similar to β-galactosidase staining, *Dll1* transcripts localize to the dorsal region of the expanded tail region and are absent from more ventral areas (Fig. 3R,S). Low levels of *Dll1* expression in the caudal halves of somites can be seen in both the *Tbx6* heterozygotes and in the partially rescued mutants (Fig. 3N-S). In addition to this mesoderm expression, *Dll1* is also expressed in neural tissue (Bettenhausen et al., 1995). *Dll1* expression is detected in the flanks of some *Tg46* rescued embryos, marking the ectopic neural tissue, which still forms in the paraxial region of some of these mutants despite the presence of paraxial somites (Fig. 3P).

We have also examined expression of other Notch signaling pathway genes in the *Tbx6* nulls and *Tg46* rescued embryos, specifically *Notch1* and lunatic fringe (*Lfng*). Although neither gene is expressed in the *Tbx6*-null embryos, the expression of both is restored in the PSM of $Tbx6^{tm1Pa}/Tbx6^{tm1Pa}$ *Tg46/+* embryos; however, this expression is reduced compared with normal embryos (data not shown). The dynamic expression of *Lfng* in the PSM was observed in the *Tg46* rescued embryos, but transcripts were present at reduced levels. The reductions in expression of the Notch signaling pathway genes *Dll1*, *Notch1* and *Lfng* in the *Tg46* rescued embryos compared with normal littermates could individually or together account for the R-C somitic defects observed.

Tbx6 genetically interacts with *rib-vertebrae*

The phenotype of the partially rescued *Tbx6* mutant embryos was reminiscent of the of the *rib-vertebrae* (*rv*) mutant phenotype. *rv* is a spontaneous recessive mutation characterized by fusions of ribs and vertebrae, shortened trunk, kinked tail, formation of a single kidney, and reduced fertility (Beckers et al., 2000b; Nacke et al., 2000; Theiler and Varnum, 1985). *rv* homozygous embryos are recognized by an enlarged tailbud, which later in development has multiple outgrowths [which are characteristics shared with the *Tg46* rescued embryos (Fig. 2D)], and by caudal duplications of the neural tube [which is a characteristic shared with the *Tbx6*-null mouse (Chapman and Papaioannou, 1998; Theiler and Varnum, 1985)]. Interestingly, *rv* had been mapped to position 62 cM on mouse chromosome 7 (Beckers et al., 2000b), which was close to the mapped location of *Tbx6* at position 61 cM (Chapman et al., 1996). Altogether, these data suggest that *Tbx6* is the gene affected in the *rv* mutation. To determine whether *Tbx6* interacts genetically with *rv*, embryos were dissected from $Tbx6^{tm1Pa}/+ \times rv/rv$ crosses at E15.5 and their skeletons were stained with Alcian Blue and Alizarin Red (Fig. 4A-E). At the level of gross morphology, compound heterozygous embryos can be distinguished by their short stature and short tails (Fig. 4B), similar to the *Tg46* rescued embryos. The genetic interaction between these two mutations is further illustrated by skeletal preparations of these embryos, which clearly show fusions of ribs and vertebrae along the entire AP axis (Fig. 4D,E). $Tbx6^{tm1Pa}/+$ *rv/+* pups are either resorbed during development or are found dead at birth. Examination of *Tbx6* expression in *rv/rv* and *rv/+* embryos revealed that although *Tbx6* was expressed in the correct spatial pattern, transcripts were present at lower levels in the tailbuds of *rv/rv* compared with *rv/+* (Fig. 4F). In addition, *Tbx6* expression is reduced in the compound mutant embryos compared with $Tbx6^{tm1Pa}/+$ (data not shown). These results indicate that *Tbx6* expression is directly affected in the *rv* mutant, and that the genetic interaction observed between the two mutants is probably due to reduced levels of *Tbx6* expression.

The strong genetic interaction between *Tbx6* and *rv* led us to identify the molecular lesion responsible for the *rv* mutation, reasoning that it was a mutation in *Tbx6*. Genomic DNA prepared from both wild-type and *rv/rv* mice was analyzed by Southern blot hybridization using a number of probes derived from the *Tbx6* locus. Polymorphisms were detected between wild-type and *rv/rv* genomic DNA (data not shown), indicating that *Tbx6* is the affected gene in the *rv* mutation. The region of *Tbx6* affected in the *rv* mutation is

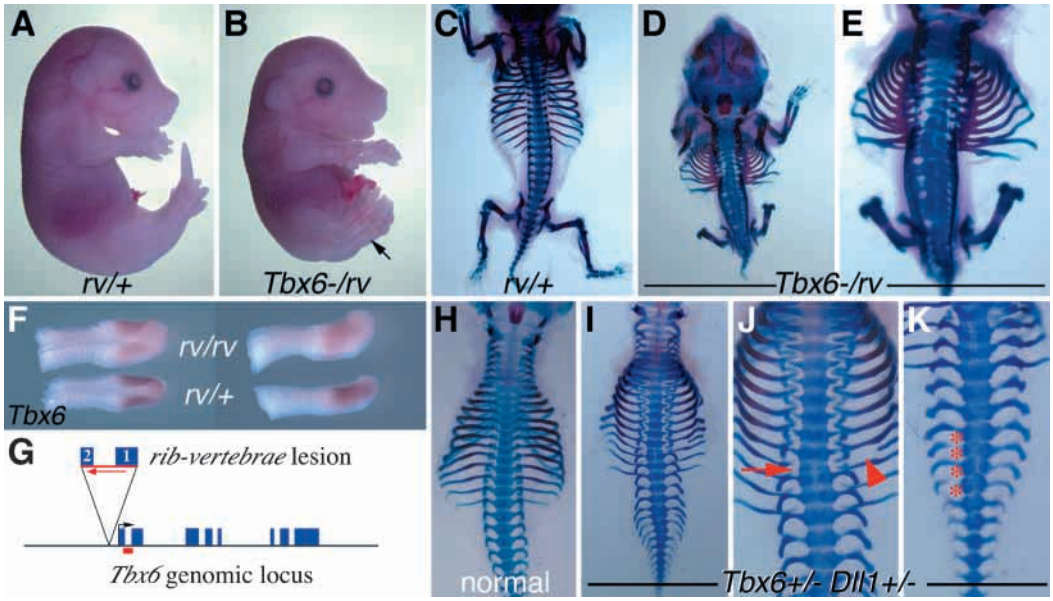

Fig. 4. Genetic interaction between *Tbx6* and *rib-vertebrae* (*rv*). The genotypes are as indicated, except where 'normal' is given to indicate that differences were not observed for embryos that were wild type, $Tbx6^{tm1Pa}$/+ or $Dll1^{tm1Gos}$+ in H. (A-E) Gross morphology and skeletal preparations of E15.5 embryos dissected from $Tbx6^{tm1Pa}$/+ × *rv/rv* matings. (A,B) $Tbx6^{tm1Pa}$/*rv* embryos are shorter in stature than their *rv*/+ littermates and have short tails (arrow in B indicates the tip of the tail). (C-E) Alcian Blue and Alizarin Red skeletal staining reveals fusions of the ribs and vertebrae along the entire AP axis of the $Tbx6^{tm1Pa}$/*rv* embryos. (E) High magnification of the skeleton in D shows that rib fusions occur both proximally and distally and that the neural arches of the lumbar region are fused along the axis. (F) *Tbx6* expression in the tail regions of *rv/rv* and *rv*/+ E10.5 embryos. Dorsal (left) and side (right) views of the tails are shown. The tailbuds of the *rv/rv* mutant embryos are larger than the *rv*/+ littermates, and show diminished levels of *Tbx6* transcripts compared with *rv*/+ tails. (G) The *Tbx6* genomic locus showing the positions of the exons (blue boxes), start of transcription (black arrow), and the position and nature of the *rv* lesion. A red line indicates the *Tbx6* genomic region that is duplicated and inverted (red arrow) in the *rv* mutation. The *rv* mutation is caused by the insertion of this duplicated and inverted region upstream of the *Tbx6*-coding region. (H-K) Alcian Blue and Alizarin Red skeletal preparations from E14.5 embryos dissected from $Tbx6^{tm1Pa}$/+ × $Dll1^{tm1Gos}$/+ crosses. (H) Heterozygous embryos for either *Tbx6* or *Dll1* showed normal skeletal morphology. (I) The genetic interaction between these two mutations can be seen in compound heterozygotes (labeled as $Tbx6^{+/-}$ $Dll1^{+/-}$), which are characterized by the presence of abnormally formed vertebrae and ribs along the AP axis. (J,K) Higher magnifications of the $Tbx6^{tm1Pa}$/+ $Dll1^{tm1Gos}$/+ skeleton in I, the thoracic and lumbar region is shown in J, and the lumbar and sacral regions are shown in K. (J) A rib missing its proximal portion is indicated by a red arrowhead. Abnormally formed vertebrae are seen in thoracic vertebrae in (J, red arrow) and in the lumbar vertebrae in (K, red asterisks). Limbs have been removed from all skeletons.

upstream of the initiating methionine within 1.2 kb of the start of transcription. PCR was used to amplify the affected region and sequencing revealed that the *rv* mutation is caused by a 185 bp insertion of a duplicated region of the *Tbx6* gene (Fig. 3G). This duplication, which includes a region of the first exon, the entire first intron and a region of the second exon, is inverted with respect to the endogenous gene and inserted into the presumed enhancer region of *Tbx6*. The location of the *rv* lesion, together with the reduced *Tbx6* expression in tailbuds of *rv/rv* versus *rv*/+ embryos, suggests that this mutation somehow affects the ability of this enhancer element to function properly, and therefore *rv* is a hypomorphic allele of *Tbx6*.

The defect in somite formation in *rv/rv* mice is due to disruption of R-C patterning of the somites and this ultimately leads to the fusions of ribs and vertebrae (Beckers et al., 2000b; Nacke et al., 2000). *rv* genetically interacts with *Dll1* (Beckers et al., 2000b; Nacke et al., 2000). As we have identified *rv* as an allele of *Tbx6*, the targeted mutant allele of *Tbx6* ($Tbx6^{tm1Pa}$) should also interact genetically with *Dll1*. We confirmed this by generating $Tbx6^{tm1Pa}$/+ $Dll1^{tm1Gos}$/+ embryos and mice. Examination of the $Tbx6^{tm1Pa}$/+ $Dll1^{tm1Gos}$/+ embryonic skeletons revealed a variety of vertebral defects, including fusions of the neural arches in cervical vertebrae, missing regions of ribs and abnormally formed vertebrae along the AP axis (Fig. 4I-K). $Tbx6^{tm1Pa}$/+ $Dll1^{tm1Gos}$/+ mice are born and can be distinguished by their kinked tails (not shown). The phenotypes of these compound heterozygotes were much milder than those seen for either the *Tg46* rescued embryos or the $Tbx6^{tm1Pa}$/*rv* mutant embryos described above.

Defects in myotome in *Tbx6* hypomorphic embryos

Whether reduced *Tbx6* expression in the embryo is achieved by transgene rescue of the *Tbx6*-null or by a bona fide *Tbx6* hypomorphic mutation, patterning of the myotome compartment of the somite is also clearly disrupted. Marker gene analysis of the $Tbx6^{tm1Pa}$/$Tbx6^{tm1Pa}$ *Tg46*/+ and $Tbx6^{tm1Pa}$/*rv* embryos revealed irregular patterning of the myotome in these mutant embryos (Fig. 5). Myogenin is normally expressed in distinct stripes along the AP axis, marking the myotome (Cheng et al., 1992; Sassoon et al., 1989; Wright et al., 1989) (Fig. 5A,C). In both the $Tbx6^{tm1Pa}$/$Tbx6^{tm1Pa}$ *Tg46*/+ and the $Tbx6^{tm1Pa}$/*rv* embryos, myogenin expression no longer has an evenly spaced striped pattern, but instead has areas of fused adjacent myotomes, as well as isolated pools of myogenin-expressing cells along the AP axis (Fig. 5B,D). Defects in these *Tbx6* hypomorphs therefore affect multiple compartments of the somite.

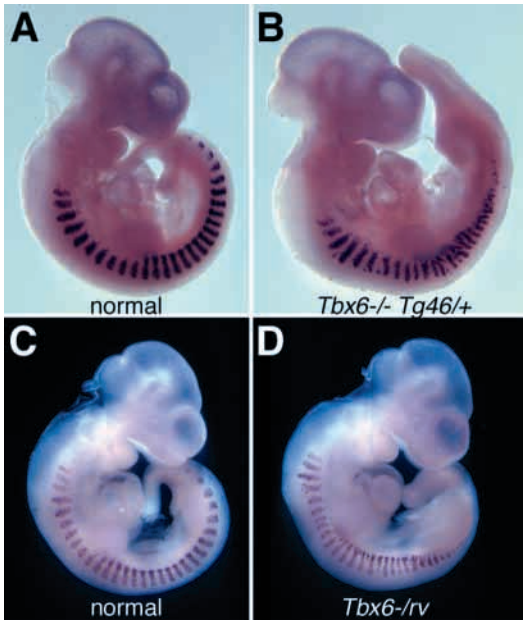

Fig. 5. Whole-mount in situ hybridization of myogenin expression in embryos with reduced *Tbx6* expression. Embryos were dissected at E10.5 from crosses of *Tbx6*^{tm1Pa}/+ *Tg46*/+ × *Tbx6*^{tm1Pa}/+ (A,B) and *Tbx6*^{tm1Pa}/+ × *rv/rv* (C,D) mice, and hybridized with a myogenin antisense riboprobe. The designation 'normal' is given to embryos that were either wild type or *Tbx6*^{tm1Pa}/+ with or without the *Tg46* transgene (A), or *rv*/+ (C), which showed no differences in myogenin expression compared with wild-type embryos. (A,C) Myogenin is normally expressed in the myotome compartment of the differentiating somite and thus appears as evenly spaced stripes along the AP axis. Expression of myogenin in either the *Tbx6*^{tm1Pa}/*Tbx6*^{tm1Pa} *Tg46*/+ (B) or *Tbx6*^{tm1Pa}/*rv* (D) embryo is disorganized compared with 'normal' littermates, showing areas in which the myotomes are fused or form as small isolated islands in the intersegmental regions.

DISCUSSION

Specification of paraxial mesoderm and somitogenesis

The process of somitogenesis in mice can be temporally divided into two phases: first the specification of paraxial mesoderm from cells within the primitive streak; and, second, the division of paraxial mesoderm into somites and the generation of R-C patterning within them. Previous studies have shown that Tbx6 is required for the specification of posterior paraxial mesoderm, while other studies have shown that the correct spatial and temporal expression and activity of Notch signaling pathway components is required for somite formation and R-C patterning.

In *Tbx6*-null mutant embryos, somites posterior to the forelimb bud fail to form, and mesodermal tissue in the tails of these mutants appears to be arrested at the primitive streak stage of differentiation. It was not clear from these studies, however, if Tbx6 played any role in patterning of the somites or if it was simply required for establishing the paraxial mesoderm fate. We show that embryos with *Tbx6* expression levels intermediate between null homozygotes and heterozygotes develop somites but that these are incorrectly patterned along their R-C axis, which leads to abnormalities in somite-derived tissue, most notably the axial skeleton. These embryos were generated in two ways: first, by using a rescuing transgene containing the *Tbx6*-coding region and cis-regulatory elements in a *Tbx6* null mutant; and, second, by identifying a previously known mutation, *rv*, as a hypomorphic mutation in *Tbx6*.

Disruption of R-C somite patterning in embryos with reduced *Tbx6* expression levels

Expression studies in embryos with reduced *Tbx6* expression reveal that the R-C division is clearly disrupted. In both the *rv/rv* and *Tbx6*^{tm1Pa}/*Tbx6*^{tm1Pa} *Tg46*/+ embryos, the caudal somite compartment marker *Uncx4.1* is expressed in a wider somite domain compared with normal embryos, suggesting that somites in these embryos have adopted a caudal phenotype (Fig. 3A-D) (Beckers et al., 2000b). The degree of caudalization is correlated with the severity of the phenotypes and hence with the level of *Tbx6* expression. The low level of *Tbx6* expression observed in the *Tg46* rescued embryos results in almost complete caudalization of the somites (as assessed by *Uncx4.1* expression) and to severe fusions of the ribs and vertebrae along the entire AP axis of the embryo. In *rv/rv* embryos, intermediate levels of *Tbx6* (between the *Tg46* rescued embryos and *Tbx6* heterozygotes) result in somites with wider than normal domains of *Uncx4.1* expression; however, unstained regions in these somites were also observed (Beckers et al., 2000b). Consequently, the rib and vertebral fusions were not as severe in the *rv/rv* embryos compared with *Tg46* rescued embryos (Fig. 2I) (Beckers et al., 2000b). Although somites in the *Tg46* rescued embryos appear caudalized, marker genes specific for the rostral compartment of the forming somite, such as *Mesp2, Cer1* and *Tbx18*, are still present. *Mesp2* marks the rostral half of the forming somite and plays a role in specifying rostral somite compartment identity, as paraxial mesoderm in the *Mesp2* homozygous mutant embryos becomes caudalized (Saga et al., 1997). *Mesp2* is still expressed in *Tg46* rescued embryos and suggests that rostral somite identity is initially established in these embryos; however, it is eventually lost, based on *Uncx4.1* expression. This result is supported by the expression of another rostral somite marker, *Cer1*. *Cer1* is expressed in the anterior PSM of the *Tg46* rescued embryos, but is expressed at low levels and is not expressed in a third stripe in the most recently formed somite, again supporting an eventual loss of rostral compartment identity. In this regard, our data for *Cer1* expression in the *Tbx6*^{tm1Pa}/*Tbx6*^{tm1Pa} *Tg46*/+ embryos differs from that previously reported for the *rv/rv* mutant embryos, where *Cer1* expression was shown to be absent (Beckers et al., 2000b). It is unclear why this difference was observed between the *rv/rv* and *Tbx6*^{tm1Pa}/*Tbx6*^{tm1Pa} *Tg46*/+ embryos, especially as the rostral marker *Mesp2* was expressed in the *rv/rv* embryos, indicating that the rostral compartment is formed. Further analysis of rostral somite compartment identity revealed that *Tbx18*, which is normally expressed in the rostral halves of somites along the AP axis of the embryo, is either not expressed or is expressed at lower levels in the most recently formed somites, and is lost in more anterior somites of the *Tg46* rescued embryos. The irregular R-C somite patterning is further exemplified by neurofilament L expression in the neural crest-derived spinal ganglia, which normally

appear as discrete segments along the AP axis because of their migration through the rostral halves of somites. In our *Tg46* rescued embryos, neurofilament L expression appears disorganized with segments fusing.

Segmentation of the PSM is believed to be dependent on these R-C differences (Stern and Keynes, 1987). Clear somite boundaries appear to be established in embryos with reduced levels of *Tbx6*, suggesting that some differences in R-C compartments are initially established in these embryos. These R-C differences, however, are not sufficiently maintained, as demonstrated by *Tbx18* and neurofilament L expression patterns. The failure to establish firmly and/or maintain R-C differences lead to later defects in resegmentation, which can account for the vertebral defects observed. Although the myotome is not directly dependent on R-C patterning of the somite, the myotome is affected in the *Tbx6* hypomorphs. Our results suggest therefore that the failure to maintain these R-C differences will indeed affect other compartments of the somite, perhaps because of a failure to maintain somite boundaries.

Dll1, a potential target of Tbx6

The disruption in somite patterning observed in embryos with reduced levels of *Tbx6* is similar to that of Notch signaling component mutants, suggesting that the expression or activity of one or more genes involved in this pathway is disrupted in the presomitic mesoderm of these embryos. The Notch ligand *Dll1* is an obvious candidate, because expression is completely lost in the *Tbx6*-null embryo (Chapman and Papaioannou, 1998). *Dll1* expression is restored in *Tg46* rescued embryos, but the level of *Dll1* transcripts is clearly reduced compared with that in *Tbx6* heterozygotes. Furthermore, previous studies with *rv* and our studies here with the *Tbx6*-null allele have revealed a strong genetic interaction between *Dll1* and *Tbx6*: $Tbx6^{tm1Pa}$/+ $Dll1^{tm1Gos}$/+ embryos have defects in rib and vertebral patterning, although this phenotype is much weaker than *rv/rv* or $Tbx6^{tm1Pa}/Tbx6^{tm1Pa}$ *Tg46*/+. Thus, one likely cause for the defective somite patterning in embryos with reduced levels of *Tbx6* is a reduction in *Dll1* expression. As demonstrated by gene targeting experiments, *Dll1* is required for proper R-C patterning of the somites and for epithelialization of the somites (Hrabe de Angelis et al., 1997).

Dll3 expression in embryos with reduced *Tbx6* expression is indistinguishable from wild type, indicating that there is not a simple reduction in expression of all presomitic-specific genes in these embryos. Consistent with this, no genetic interaction between *Dll3* and *rv* was detected (Beckers et al., 2000b). *Notch1* and *Lfng*, which are also required for somite formation and patterning, are expressed at reduced levels in the PSM of these embryos, but in the correct spatial patterns. The reduced expression levels of these genes might contribute to the observed phenotypes. However, no genetic interaction between *Notch1* and *rv* was detected (Beckers et al., 2000b), again implicating Dll1 as the primary factor disrupted in these embryos.

One problem with directly linking *Tbx6* and *Dll1* is that the mutants appear to have opposite phenotypes in terms of their effects on compartmentalization of the somites. In *Dll1*-null mutants, somites appear to be rostralized (Barrantes et al., 1999), in contrast to their caudalization in embryos with reduced levels of *Tbx6*. At present, the reason for this is not clear. It is likely that Tbx6 is regulating the expression of other genes besides *Dll1*, as would be expected based on the differences in the *Tbx6* and *Dll1* null phenotypes. Other likely candidates are *Notch1* and *Lfng*, the expression of which was restored in embryos expressing lowered levels of *Tbx6* compared with their lack of expression in the homozygous null. The combined effects of lowered *Dll1*, *Notch1* and *Lfng* may account for the differences seen in compartment phenotypes. A complete explanation awaits the identification of these additional Tbx6 targets. Another explanation is that reduction rather than complete loss of Dll1 may result in caudalization rather than rostralization: this can only be tested directly with *Dll1* hypomorphs.

Tbx6 is a transcription factor and thus could be directly activating *Dll1*. The regulatory elements necessary for *Dll1* expression have been identified through transgenic studies (Beckers et al., 2000a). We have examined these regulatory elements for T-box-binding sites using the binding site identified for T (Kispert and Herrmann, 1993); however, no palindromic or half sites were identified. As the binding site for Tbx6 has not yet been identified, further analysis along these lines awaits the identification of a Tbx6-specific binding site.

Human disorders caused by *Tbx6* mutations?

Mouse embryos that bear homozygous *Tbx6*-null mutations result in a lethal phenotype by embryonic day 12.5 (Chapman and Papaioannou, 1998). It is likely that similar mutations in humans would also lead to early embryonic lethal phenotypes that would probably appear as spontaneous abortions. Mice heterozygous for the *Tbx6* mutation are normal and fertile, with no signs of skeletal or muscle abnormalities, suggesting that humans heterozygous for *Tbx6*-null mutations would presumably be normal. This paper identifies phenotypes that lie between these two extremes, with hypomorphic levels of *Tbx6* expression resulting in R-C patterning defects in the somites. Thus far, no human syndromes that would result from improper R-C somite patterning map to human *TBX6* on chromosome 16. However, several syndromes like Klippel-Feil and spondylocostal and spondylothoracic dysostosis, which display a number of clinical defects including rib and vertebral fusions, may in the future be linked to hypomorphic mutations in *TBX6* or to genes functioning in this pathway.

We thank S. Dunwoodie, Y. Saga, A. Kispert, M. Maconochie, R. Behringer, A. Gossler, Anita Myer and W. Klein for gifts of plasmids, and Jeffrey Hildebrand and Gerard Campbell for helpful discussions. This work was supported by a grant from the NIH (HD38786).

REFERENCES

Barrantes, I. B., Elia, A. J., Wunsch, K., de Angelis, M. H., Mak, T. W., Rossant, J., Conlon, R. A., Gossler, A. and de la Pompa, J. L. (1999). Interaction between notch signalling and lunatic fringe during somite boundary formation in the mouse. *Curr. Biol.* **9**, 470-480.

Beckers, J., Caron, A., Hrabe de Angelis, M., Hans, S., Campos-Ortega, J. A. and Gossler, A. (2000a). Distinct regulatory elements direct Delta1 expression in the nervous system and paraxial mesoderm of transgenic mice. *Mech. Dev.* **95**, 23-34.

Beckers, J., Schlautmann, N. and Gossler, A. (2000b). The mouse rib-vertebrae mutation disrupts anterior-posterior somite patterning and genetically interacts with a delta1 null allele. *Mech. Dev.* **95**, 35-46.

Bettenhausen, B., Hrabe de Angelis, M., Simon, D., Guenet, J. L. and

Gossler, A. (1995). Transient and restricted expression during mouse embryogenesis of Dll1, a murine gene closely related to Drosophila Delta. *Development* **121**, 2407-2418.

Biben, C., Stanley, E., Fabri, L., Kotecha, S., Rhinn, M., Drinkwater, C., Lah, M., Wang, C. C., Nash, A., Hilton, D. et al. (1998). Murine cerberus homologue mCer-1: a candidate anterior patterning molecule. *Dev. Biol* **194**, 135-151.

Bronner-Fraser, M. (2000). Rostrocaudal differences within the somites confer segmental pattern to trunk neural crest migration. *Curr. Top. Dev. Biol.* **47**, 279-296.

Bulman, M. P., Kusumi, K., Frayling, T. M., McKeown, C., Garrett, C., Lander, E. S., Krumlauf, R., Hattersley, A. T., Ellard, S. and Turnpenny, P. D. (2000). Mutations in the human delta homologue, DLL3, cause axial skeletal defects in spondylocostal dysostosis. *Nat. Genet.* **24**, 438-441.

Chapman, D. L. and Papaioannou, V. E. (1998). Three neural tubes in mouse embryos with mutations in the T-box gene Tbx6. *Nature* **391**, 695-697.

Chapman, D. L., Agulnik, I., Hancock, S., Silver, L. M. and Papaioannou, V. E. (1996). Tbx6, a mouse T-box gene implicated in paraxial mesoderm formation at gastrulation. *Dev. Biol.* **180**, 534-542.

Cheng, T. C., Hanley, T. A., Mudd, J., Merlie, J. P. and Olson, E. N. (1992). Mapping of myogenin transcription during embryogenesis using transgenes linked to the myogenin control region. *J. Cell Biol.* **119**, 1649-1656.

Christ, B., Huang, R. and Wilting, J. (2000). The development of the avian vertebral column. *Anat. Embryol.* **202**, 179-194.

Ciruna, B. G., Schwartz, L., Harpal, K., Yamaguchi, T. P. and Rossant, J. (1997). Chimeric analysis of fibroblast growth factor receptor-1 (Fgfr1) function: a role for FGFR1 in morphogenetic movement through the primitive streak. *Development* **124**, 2829-2841.

Dunwoodie, S. L., Clements, M., Sparrow, D. B., Sa, X., Conlon, R. A. and Beddington, R. S. (2002). Axial skeletal defects caused by mutation in the spondylocostal dysplasia/pudgy gene Dll3 are associated with disruption of the segmentation clock within the presomitic mesoderm. *Development* **129**, 1795-1806.

Dunwoodie, S. L., Henrique, D., Harrison, S. M. and Beddington, R. S. (1997). Mouse Dll3: a novel divergent Delta gene which may complement the function of other Delta homologues during early pattern formation in the mouse embryo. *Development* **124**, 3065-3076.

Hogan, B., Beddington, R., Costantini, F. and Lacy, E. (1994). *Manipulating the Mouse Embryo*. Cold Spring Harbor: Cold Spring Harbor Laboratory Press.

Hrabe de Angelis, M., McIntyre, J., 2nd and Gossler, A. (1997). Maintenance of somite borders in mice requires the Delta homologue DII1. *Nature* **386**, 717-721.

Huang, R., Zhi, Q., Neubuser, A., Muller, T. S., Brand-Saberi, B., Christ, B. and Wilting, J. (1996). Function of somite and somitocoele cells in the formation of the vertebral motion segment in avian embryos. *Acta Anat.* **155**, 231-241.

Kispert, A. and Herrmann, B. G. (1993). The Brachyury gene encodes a novel DNA binding protein. *EMBO J.* **12**, 3211-3220.

Kraus, F., Haenig, B. and Kispert, A. (2001). Cloning and expression analysis of the mouse T-box gene Tbx18. *Mech. Dev.* **100**, 83-86.

Lewis, S. A. and Cowan, N. J. (1985). Genetics, evolution, and expression of the 68,000-mol-wt neurofilament protein: isolation of a cloned cDNA probe. *J. Cell Biol.* **100**, 843-850.

Mansouri, A., Yokota, Y., Wehr, R., Copeland, N. G., Jenkins, N. A. and Gruss, P. (1997). Paired-related murine homeobox gene expressed in the developing sclerotome, kidney, and nervous system. *Dev. Dyn.* **210**, 53-65.

Nacke, S., Schafer, R., Habre de Angelis, M. and Mundlos, S. (2000). Mouse mutant "rib-vertebrae" (rv): a defect in somite polarity. *Dev. Dyn.* **219**, 192-200.

Neidhardt, L., Kispert, A. and Herrmann, B. G. (1997). A mouse gene of the paired-related homeobox class expressed in the caudal somite compartment and in the developing vertebral column, kidney and nervous system. *Dev. Genes Evol.* **207**, 330-339.

Pourquie, O. and Kusumi, K. (2001). When body segmentation goes wrong. *Clin. Genet.* **60**, 409-416.

Saga, Y. and Takeda, H. (2001). The making of the somite: molecular events in vertebrate segmentation. *Nat. Rev. Genet.* **2**, 835-845.

Saga, Y., Hata, N., Koseki, H. and Taketo, M. M. (1997). Mesp2: a novel mouse gene expressed in the presegmented mesoderm and essential for segmentation initiation. *Genes Dev.* **11**, 1827-1839.

Sassoon, D., Lyons, G., Wright, W. E., Lin, V., Lassar, A., Weintraub, H. and Buckingham, M. (1989). Expression of two myogenic regulatory factors myogenin and MyoD1 during mouse embryogenesis. *Nature* **341**, 303-307.

Shawlot, W., Min Deng, J., Wakamiya, M. and Behringer, R. R. (2000). The cerberus-related gene, Cerr1, is not essential for mouse head formation. *Genesis* **26**, 253-258.

Stern, C. D. and Keynes, R. J. (1987). Interactions between somite cells: the formation and maintenance of segment boundaries in the chick embryo. *Development* **99**, 261-272.

Takahashi, Y., Koizumi, K., Takagi, A., Kitajima, S., Inoue, T., Koseki, H. and Saga, Y. (2000). Mesp2 initiates somite segmentation through the Notch signalling pathway. *Nat. Genet.* **25**, 390-396.

Theiler, K. and Varnum, D. S. (1985). Development of rib-vertebrae: a new mutation in the house mouse with accessory caudal duplications. *Anat. Embryol.* **173**, 111-116.

Wilkinson, D. G. (1992). Whole mount in situ hybridization of vertebrate embryos. In *In Situ Hybridization: A Practical Approach* (ed. D. G. Wilkinson), pp. 75-83. Oxford: IRL Press.

Wright, W. E., Sassoon, D. A. and Lin, V. K. (1989). Myogenin, a factor regulating myogenesis, has a domain homologous to MyoD. *Cell* **56**, 607-617.